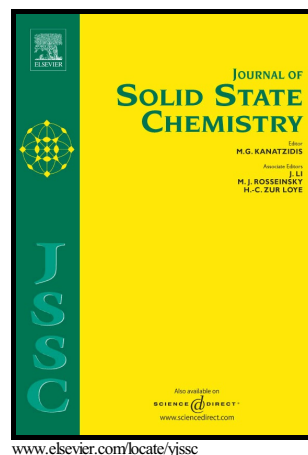


## Author's Accepted Manuscript

( $\mu$ -O, $O'$ )-nitrito bridged 3-D coordination frameworks of  $M^{2+}$  (Mn Co, Zn) with mab and jsm topology

Rima Paul, Ankur K. Guha, Lakshi Saikia, Sanchay J. Bora



PII: S0022-4596(17)30291-8  
DOI: <http://dx.doi.org/10.1016/j.jssc.2017.07.031>  
Reference: YJSSC19881

To appear in: *Journal of Solid State Chemistry*

Received date: 25 May 2017  
Revised date: 4 July 2017  
Accepted date: 27 July 2017

Cite this article as: Rima Paul, Ankur K. Guha, Lakshi Saikia and Sanchay J Bora, ( $\mu$ -O, $O'$ )-nitrito bridged 3-D coordination frameworks of  $M^{2+}$  (Mn Co, Zn) with mab and jsm topology, *Journal of Solid State Chemistry*, <http://dx.doi.org/10.1016/j.jssc.2017.07.031>

This is a PDF file of an unedited manuscript that has been accepted for publication. As a service to our customers we are providing this early version of the manuscript. The manuscript will undergo copyediting, typesetting, and a review of the resulting galley proof before it is published in its final citable form. Please note that during the production process errors may be discovered which could affect the content, and all legal disclaimers that apply to the journal pertain

**( $\mu$ -O,O')-nitrito bridged 3-D coordination frameworks of  $M^{2+}$  (Mn Co, Zn)  
with mab and jsn topology**

Rima Paul,<sup>a</sup> Ankur K. Guha,<sup>b</sup> Lakshi Saikia<sup>c</sup> and Sanchay J. Bora<sup>\*a</sup>

<sup>a</sup>Department of Chemistry, Pandu College, Guwahati-781012, Assam, India

<sup>b</sup>Department of Chemistry, Gauhati University, Guwahati-781014, Assam, India

<sup>c</sup>Materials Science Division, North-East Institute of Science and Technology, Jorhat-785006, Assam, India

Tel: +91-361-2570450, E-mail:sanchay.bora@gmail.com

### Abstract

Four new nitrito-bridged coordination polymers of formulation  $[Zn(NO_2)_2(H_2O)_2]_n$  (**1**) and  $[M(bipy)(NO_2)_2]_n$  [M= Zn (**2**), Co (**3**), Mn (**4**)] were synthesized under solvothermal condition using N,N-dimethylformamide (DMF) as a reducing solvent. Theoretical calculation suggests *in situ* reduction of nitrate to nitrite with high spontaneity and without any thermodynamic barrier ( $\Delta G = -20.4$  kcal/mol). All the complexes were characterized by elemental analysis, FT-IR spectroscopy, UV-vis spectroscopy, Raman Spectroscopy, TG analysis as well as by single crystal X-ray diffraction methods. TD-DFT approach has been employed to assign the electronic transitions occurring in the cobalt(II) complex (**3**) and were compared with those observed experimentally. This work also describes the preliminary studies on heterogeneous oxidation of cyclohexene by **2** & **3** in acetonitrile medium using TBHP.

*Keywords: Nitrito-bridged coordination polymer, solvothermal synthesis, topological analysis, isostructurality, TD-DFT*

---

### 1. Introduction

The fascinating structural diversities of inorganic coordination polymers (CPs) [1-6], coupled with their specific functionality have made them excellent candidates for various potential applications[7-13] such as heterogeneous catalysis, gas and liquid adsorption, nonlinear optics, magnetism, and molecular recognition. These polymeric complexes are often generated from relatively simple subunits, wherein the nature of the metal ion and the coordinating ability of the inorganic/organic ligands (linkers) play an important role in

the self assembly process. An effective strategy to assemble these functional CPs is to use different polyatomic ligands which include N- or O-coordinating molecules to connect the metal ions or clusters (nodes) [14-17]. In this context, the nitrite group ( $\text{NO}_2^-$ ) is regarded as unique among the short ligands because of the number of ways in which it can coordinate to the metal ion [18-21]. It possesses diverse bridging capabilities and have been employed as inorganic linkers to construct mono-, di- or poly-nuclear coordination polymers with different dimensionalities. For example, as an ambidentate ligand,  $\text{NO}_2^-$  can coordinate either through N- or O-atom, while as a bidentate ligand, it can chelate or bridge between the metal centers. The chelation or bridge is possible either through N- and O- atoms or through O-atoms only. However, to the best of our knowledge, only a handful of 2-D or 3-D polymeric compounds containing  $\mu_{1,3}$ -nitrito bridges have been reported so far. Most of them were constructed using paramagnetic metal ions with a view of examining their detail magnetic properties [22, 23]. No reports have been made with such coordination polymers showing catalytic properties. In addition, aromatic N-donor auxiliary ligands that can compete with the parent ligand in coordination may also be introduced to bring about substantial structural tuning of the polymer [24-26]. The rod like linear *N,N*-donor ligand, 4,4'-bipyridine (bipy) is often used in the construction of multi-dimensional CPs involving 1-D ladder [27-30], molecular bilayer [31,32], square or rectangular grid [33-36] frameworks etc for their unique functional behaviour. In this study, we have synthesized four new nitrito- bridged coordination polymers and their catalytic activity towards cyclohexene oxidation has been explored.

## 2. Experimental

Materials used in this work were obtained from commercial sources and used without further purification.  $\text{Zn}(\text{NO}_3)_2 \cdot 6\text{H}_2\text{O}$  (Merck, India), 4,4'-bipyridine (Sigma Aldrich, USA),  $\text{Co}(\text{NO}_3)_2 \cdot 6\text{H}_2\text{O}$  (Merck, India). C,H,N analyses were done using a Perkin-Elmer 2400 Series II CHNS/O analyzer. While cobalt was estimated gravimetrically by precipitating out cobalt as  $\text{Hg}[\text{Co}(\text{NCS})_4]$  following standard procedure, zinc was determined *via* complexometric titrations. Thermogravimetric (TG) data were obtained using a Mettler Toledo TGA/DSC1 STAR<sup>c</sup> system in the 40-800°C range. Thermal decompositions of all the complexes were studied under  $\text{N}_2$  atmosphere at a heating rate of 10°C min<sup>-1</sup>. FT-IR spectra were recorded on a Perkin-Elmer RX1 spectrophotometer in the mid-IR region (4000 to 450 cm<sup>-1</sup>) for KBr pellets. The UV-vis-NIR (240-2600 nm) diffuse-reflectance spectra were obtained using a Hitachi U-4100 spectrophotometer. Raman spectra were recorded on a Horiba Jobin Vyon, Model LabRam HR system in the range 50-1800 cm<sup>-1</sup>. Room temperature magnetic susceptibilities were measured at 300K on a Sherwood Mark 1 Magnetic Susceptibility Balance by Evans Method.

### 2.1. Preparation of $[\text{Zn}(\text{NO}_2)_2(\text{H}_2\text{O})_2]_n \mathbf{I}$

0.297 g (1 mmol) of zinc nitrate hexahydrate  $\text{Zn}(\text{NO}_3)_2 \cdot 6\text{H}_2\text{O}$  was dissolved in 10mL DMF placed in a stainless steel vessel, which was sealed and placed in programmable oven. The mixture was heated at 120°C at 5°C/min and held at that temperature for 24hr followed by further cooling at room temperature. The resulting colourless crystals were filtered, washed with methanol and then dried in a vacuum desiccator over fused  $\text{CaCl}_2$ . Yield:68%. Anal. Calcd. for  $\text{N}_4\text{H}_8\text{O}_{12}\text{Zn}_2$ : H, 2.05%; N, 14.50%; Zn, 33.82%. Found: H, 2.29%; N, 14.88%; Zn, 33.01%. IR spectral data (KBr disc, cm<sup>-1</sup>): 3431(br), 2924(m), 2851(m), 2793(w), 2496(w), 2363(m), 1595(s), 1458(m), 1342(s), 1256(w), 1103(m), 1026(m), 986(w), 897(w), 802(s), 604(m). [s, strong; m, medium; w, weak; br, broad ].

## 2.2. Preparation of $[Zn(bipy)(NO_2)_2]_n$ **2**

0.297 g (1 mmol) of zinc nitrate hexahydrate  $Zn(NO_3)_2 \cdot 6H_2O$  and 4,4'-bipyridine ( $C_{10}H_8N_2$ ) (0.312g, 2mmol) was dissolved in 10mL DMF placed in a stainless steel vessel, which was sealed and placed in programmable oven. The mixture was heated at  $120^\circ C$  at  $5^\circ C/min$  and held at that temperature for 24hr followed by further cooling at room temperature. The resulting colourless crystals were filtered, washed with methanol and then dried in a vacuum desiccator over fused  $CaCl_2$ . Yield: 75%. Anal. calcd. for  $C_{10}H_8N_4O_4Zn$ : C, 38.33%; H, 2.57%; N, 17.89%; Zn, 20.85%. Found: C, 37.79%; H, 2.13%; N, 18.21%; Zn, 19.96%. IR spectral data (KBr disc,  $cm^{-1}$ ): 3422(br), 3055(w), 2922(m), 2849(m), 2762(w), 2369(m), 2344(m), 1969(w), 1611(s), 1558(s), 1389(s), 1350(s), 1221(w), 1090(w), 1015(w), 988(w), 870(w), 831(m), 777(s), 737(w), 637(s), 573(w), 527(m).

## 2.3. Preparation of $[Co(bipy)(NO_2)_2]_n$ **3**

0.291 g (1mmol) of cobalt nitrate hexahydrate  $Co(NO_3)_2 \cdot 6H_2O$  and 4,4'-bipyridine ( $C_{10}H_8N_2$ ) (0.312g, 2mmol) was dissolved in 10mL DMF placed in a stainless steel vessel, which was sealed and placed in programmable oven. The mixture was heated at  $120^\circ C$  at  $5^\circ C/min$  and held at that temperature for 24hr followed by further cooling at room temperature. The resulting rod-like pink crystals were filtered, washed with water and then dried in a vacuum desiccator over fused  $CaCl_2$ . Yield: 82%. Anal. Calcd. For  $C_{10}H_8N_4O_4Co$ : C, 39.11%; H, 2.63%; N, 18.24%; Co, 19.18%. Found: C, 39.66%; H, 2.11%; N, 18.93%; Co, 18.70%.  $\mu_{eff} = 5.02$  BM. IR spectral data (KBr disc,  $cm^{-1}$ ): 3420(br), 2922(m), 2859(m), 2766(w), 2363(w), 2344(w), 1967(w), 1609(s), 1560(s), 1389(s), 1348(s), 1221(w), 1090(w), 1013(m), 988(w), 870(w), 831(s), 779(s), 739(w), 635(s), 575(w), 527(s).

#### 2.4. Preparation of $[Mn(bipy)(NO_2)_2]_n$ **4**

0.251 g (1mmol) of manganese nitrate tetrahydrate  $Mn(NO_3)_2 \cdot 4H_2O$  and 4,4'-bipyridine ( $C_{10}H_8N_2$ ) (0.312g, 2mmol) was dissolved in 10mL DMF placed in a stainless steel vessel, which was sealed and placed in programmable oven. The mixture was heated at  $120^\circ C$  at  $5^\circ C/min$  and held at that temperature for 24hr followed by further cooling at room temperature. The resulting light brown coloured crystals were filtered, washed with water and then dried in a vacuum desiccator over fused  $CaCl_2$ . Yield: 68%. Anal. Calcd. For  $C_{10}H_8N_4O_4Mn$ : C, 39.12%; H, 2.64%; N, 18.49%. Found: C, 38.10%; H, 2.05%; N, 17.56%; IR spectral data (KBr disc,  $cm^{-1}$ ): 3408(br), 2954(w), 2841(w), 2706(w), 2374(w), 1603(s), 1533(w), 1414(m), 1391(m), 1352(m), 1221(m), 1140(w), 1076(w), 1045(w), 1004(m), 864(w), 816(s), 752(m), 734(m), 658(w), 629(s), 498(m).

#### 2.5 Computational Details

The complex has been fully optimized at B3LYP [37, 38] level of theory using 6-311++G\*\* basis set. Analytical frequency calculation has been performed at the same level of theory to characterize the nature of the stationary state. All molecules are found to be in local minimum with all real frequencies. There is a very good agreement between the calculated geometrical parameters with the experimental X-ray data. The UV-Vis spectra has been calculated at the same level of theory using methanol as the solvent medium by employing polarizable continuum model (PCM) [39]. All calculations are performed using Orca [40] suite of program.

#### 2.6 Catalysis

In a typical methodology, 2 mmol of cyclohexene was taken in 10 ml of acetonitrile in a 25 ml double necked round bottom flask fitted with water condenser to which catalyst was added at a

time. Then 2 equivalent of aqueous TBHP was added to the reaction mixture slowly. The progress of the reaction was monitored by Gas Chromatograph (ThermoFischer Trace 1300) by taking out reaction mixture through syringe at regular interval.

### 2.7 X-ray Crystallographic Procedures

Suitable crystals of compounds **1-4** for single crystal X-ray diffraction work were obtained by solvothermal process. In each case the chosen crystal was mounted on a glass fiber for intensity data collection at room temperature using graphite monochromatised Mo-K $\alpha$  radiation on a Bruker SMART CCD Diffractometer [41]. Crystal structures were solved by the direct methods (SHELXS) and refined by full-matrix least squares techniques (SHELXL) using SHELX-97 [42] from within WinGX [43]. The hydrogen atoms of aqua ligands in **1** were located in difference Fourier maps and refined with isotropic atomic displacement parameters. In order to avoid distortion in one of the coordinated water molecule (O6), the following lengths were restrained using SHLXL DFIX instructions. The bond lengths, O6–H6A and O6–H6B were restrained to be 0.99 Å and 0.86 Å respectively with the e.s.d. value of 0.02 for each. On the other hand, the hydrogen atoms of **2** and **3** are placed in calculated positions using a riding model of refinement. Crystallographic and structure refinement details are listed in Table 1. The structural diagrams were drawn using ORTEP-III [44] for Windows [45], PLUTON [46], Diamond [47] and Mercury [48].

Powder X-ray diffraction patterns in the 3–60°  $2\theta$ -range were recorded on a Philips X'Pert PRO instrument using Cu-K $\alpha$  radiation (1.5418 Å) at a scan rate of 0.5 sec (0.5°  $2\theta$ ) per step at 40 KV/30 mA. The calculated diffraction patterns assuming Bragg-Brentano geometry were obtained from results of single crystal structure analyses using the computer program PowderCell [49].

**Table 1.** Crystallographic and structure refinement data.

Details	[Zn(NO <sub>2</sub> ) <sub>2</sub> (H <sub>2</sub> O) <sub>2</sub> ] <sub>n</sub>	[Zn(bipy)(NO <sub>2</sub> ) <sub>2</sub> ] <sub>n</sub>	[Co(bipy)(NO <sub>2</sub> ) <sub>2</sub> ] <sub>n</sub>	[Mn(bipy)(NO <sub>2</sub> ) <sub>2</sub> ] <sub>n</sub>
Empirical formula	<b>1</b>	<b>2</b>	<b>3</b>	<b>4</b>
Formula weight	H <sub>4</sub> N <sub>2</sub> O <sub>6</sub> Zn	C <sub>20</sub> H <sub>16</sub> N <sub>8</sub> O <sub>8</sub> Zn <sub>2</sub>	C <sub>20</sub> H <sub>16</sub> N <sub>8</sub> O <sub>8</sub> Co <sub>2</sub>	C <sub>20</sub> H <sub>16</sub> N <sub>8</sub> O <sub>8</sub> Mn <sub>2</sub>
Temperature	193.41	627.15	614.27	606.29
Crystal system, space group	298(2)K Monoclinic, <i>P</i> 2 <sub>1</sub> / <i>c</i>	298(2)K Tetragonal, <i>P</i> 4 <sub>1</sub> 2 <sub>1</sub> 2	298(2)K Tetragonal, <i>P</i> 4 <sub>1</sub> 2 <sub>1</sub> 2	298(2)K Tetragonal, <i>P</i> 4 <sub>1</sub> 2 <sub>1</sub> 2
<i>a</i> / Å	8.680(7)	7.9719(2)	7.9805(3)	8.1510(6)
<i>b</i> / Å	7.186(5)	7.9719(2)	7.9805(3)	8.1510(6)
<i>c</i> / Å	9.276(6)	17.7528(7)	17.5253(8)	17.8407(13)
$\alpha$ / °	90.00(0)	90.0(0)	90.0(0)	90.0(0)
$\beta$ / °	97.51(5)	90.0(0)	90.0(0)	90.0(0)
$\gamma$ / °	90.00(0)	90.0(0)	90.0(0)	90.0(0)
Volume/Å <sup>3</sup>	573.6(7)	1128.21(6)	1116.16(8)	1185.32(15)
Z, Calculated density/gcm <sup>-3</sup>	4, 2.216 4.250	2, 1.846 2.194	2, 1.828 1.555	2, 1.699 1.130
Absorption coefficient/mm <sup>-1</sup>	376 0.31 × 0.29 × 0.16	632 0.43 × 0.27 × 0.18	620 0.37 × 0.21 × 0.11	612 0.35 × 0.25 × 0.13
F(000)	3.60 to 30.07	2.80 to 30.07	3.61 to 29.90	3.72 to 29.99
Crystal size/ mm	-12 ≤ h ≤ 10,	-11 ≤ h ≤ 11, -	-11 ≤ h ≤ 10, -7 ≤ k ≤ 11,	-10 ≤ h ≤ 11, -4 ≤ k ≤ 11,
$\theta$ range for data collection/°	10 ≤ k ≤ 10, -12 ≤ l ≤ 13	10 ≤ k ≤ 10, -25 ≤ l ≤ 18	-20 ≤ l ≤ 24 6121/1608	-17 ≤ l ≤ 25 6532 /1724
Index ranges	5133/1622 [ <i>R</i> (int)=0.0906]	6194/1647 [ <i>R</i> (int)=0.0252]	[ <i>R</i> (int)=0.0250] Full-matrix LS on <i>F</i> <sup>2</sup>	[ <i>R</i> (int)=0.0197] Full-matrix LS on <i>F</i> <sup>2</sup>
Reflections collected/unique	Full-matrix LS on <i>F</i> <sup>2</sup>	Full-matrix LS on <i>F</i> <sup>2</sup>	1608 / 0 / 89	1724 / 0 / 89
Refinement method	1622 / 0 / 101	1647 / 0 / 89	1.116	1.182
Data / restraints / parameters	1.031 0.0452 / 0.1644	1.105 0.0284 / 0.0757	0.0271 / 0.0779 0.000	0.0286 / 0.0862 0.000
Goodness-of-fit* on <i>F</i> <sup>2</sup>	0.000	0.000	0.586 and -0.511	0.377 and -0.634
Final <i>R</i> indices† [ <i>I</i> > 2σ( <i>I</i> )]	2.178 and -4.718	0.478 and -0.428	1450008	1532392
<i>R</i> 1/ <i>wR</i> 2	1532391	1450029		
(Shift/esd) <sub>max</sub>				
Largest diff. peak and hole /e.Å <sup>-3</sup>				
CCDC Number				

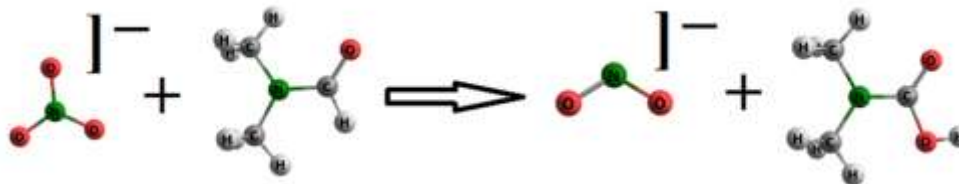
$$\dagger wR2 = \{ \sum [ w(F_o^2 - F_c^2)^2 ] / \sum [ w(F_o^2)^2 ] \}^{1/2}; R1 = \sum | |F_o| - |F_c| | / \sum |F_o|$$

$$*Goof = S = \{ \sum [ w(F_o^2 - F_c^2)^2 ] / (n-p)^2 \}^{1/2}$$

### 3. Results and Discussion

#### 3.1 Syntheses and properties

Crystals of the polymeric complexes, **1-4** have been obtained using nitrate salts of the respective metal *via* solvothermal synthesis using DMF as the solvent. The conversion of  $\text{NO}_3^-$  to  $\text{NO}_2^-$  ions in these complexes may be ascribed to the reducing property of DMF at elevated temperature. Pastoriza-Santos and co-worker had demonstrated the ability of DMF for the reduction of  $\text{Ag(I)}$  to  $\text{Ag(0)}$  even at room temperature [50]. Such a redox reaction could be possible for other metals as well while dealing with a solution of the metal in DMF. The reducing property of formamide was practiced in the syntheses of ' $\text{Ni(NO}_2)_2$ ' complexes from  $\text{Ni(NO}_3)_2$  salts as described by Vo *et al.* [23]. In the present work, DMF reduces  $\text{NO}_3^-$  ions and oxidises itself to the corresponding acid, which is believed to be taking place *via* a mechanism (Scheme 1) similar to the earlier report. TD-DFT calculation also supports the spontaneity of the reaction with  $\Delta G$  value of -20.4 kcal/mol and suggests that there is no thermodynamic barrier for the formation of the  $\text{NO}_2^-$  ion, which will bind effectively to the metal fragment during complexation.



Scheme 1

All these complexes are insoluble in water and other common organic solvents. They are non-hygroscopic and compositionally stable in air at room temperature for extended period of time.

### 3.2 Crystal Structures

#### 3.2.1 $[Zn(NO_2)_2(H_2O)_2]_n$ **1**

Single crystal X-ray diffraction analysis reveals that **1** crystallizes in monoclinic  $P2_1/c$  space group. The asymmetric unit consists of two crystallographically independent  $Zn^{2+}$  cations [Zn(1) & Zn(2)], two  $NO_2^-$  ligands and two coordinated water molecules. The crystallochemical formula (CCF) [51] of this species can be written as  $A_2B^2_4M^1_4$ , where B corresponds to nitrito ligand and M corresponds to aqua ligand. As shown in Fig. 1(a), the equatorial plane of the nearly octahedral Zn(1) coordination is constructed by four oxygen atoms from different bridging  $NO_2^-$  ligands that are connecting four nearby Zn(1) centers and generate layers parallel to the  $bc$ -plane. The remaining axial sites of the octahedron are once again occupied by two bridging  $NO_2^-$  ligands that extends in 3<sup>rd</sup> dimension relating two neighboring hexacoordinated Zn(2) centers whose equatorial planes are being made of four aqua oxygen atoms. Thus, the Zn(1) atoms can be considered as six-connected (6-c) nodes while the Zn(2) atoms as two-connected nodes (2-c), and the whole 3-D framework can be rationalized as a 6-c uninodal **mab** underlying net [Fig. 1 (b)] with point symbol  $4^4.6^{10}.8$  (analysis was performed with ToposPro [52] program). A perspective view of the polymeric extension of complex **1** in 3-D is presented in Fig. 2 (a). The Zn(1)–O (equatorial) distances ranging from 2.070(2) to 2.099(2) Å (Table S1 in SI) in **1** are of comparable magnitude to those of similar Ni(1)–O distances ranging from 2.075(3) to 2.083(3) Å in  $Ni(NO_2)_2$  [23]. Deviations of the L–M–L angles in both the coordination spheres from those expected for an octahedron ( $90^\circ$ ) speak about the distorted nature of the octahedron around  $Zn^{2+}$  centers. Further, the polymeric structure of **1** is stabilized by both intra- and inter-molecular hydrogen bonding interactions as shown in the Fig. 2 (b). These hydrogen bridges lead to an overall supramolecular network architecture having intricate patterns that can be rationalized by

invoking the graph set theory [53]. The *trans* aqua ligands in **1** along with the nitrito-O atoms connect via hydrogen bonds to form supramolecular chains which can be described as  $C_2^2(12)$  in graph set notation. Hydrogen bonded rings of descriptors  $R_1^2(3)$  and  $R_2^2(5)$  having periodic repetitions are also observed in the crystal structure of **1**.

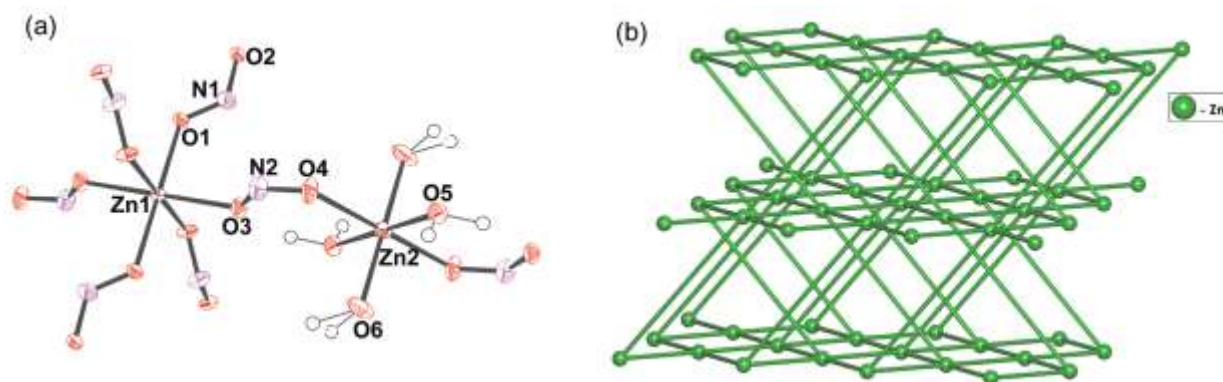


**Figure 1** a) An ORTEP presentation of polymer **1**, atoms of the asymmetric units are labelled b) a fragment of the six-connected **mab** underlying net observed in the crystal structure of **1**.

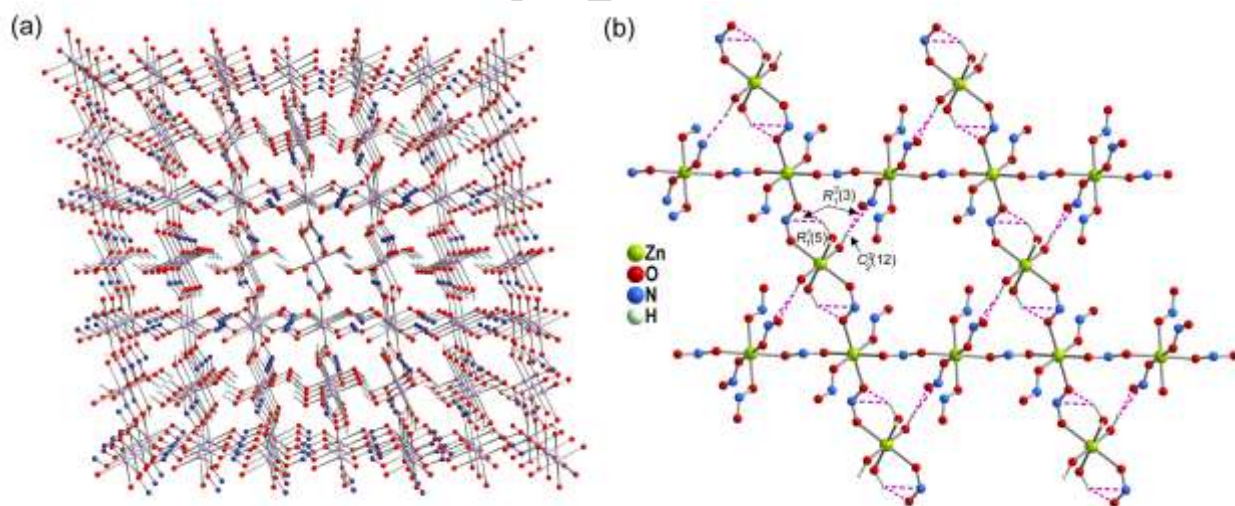


**Figure 2** a) Perspective view along the *b*-axis showing the extension of polymeric structure in 3-D b) intra- and inter- molecular hydrogen bridges present in the crystal structure of **1**.

### 3.2.2 $[M(\text{bipy})(\text{NO}_2)_2]_n$ [ $M = \text{Zn}$ for **2**; $\text{Co}$ for **3** and $\text{Mn}$ for **4**]

Single crystal X-ray diffraction analysis indicates that the complexes **2** [ $\text{Zn}^{2+}$ ], **3** [ $\text{Co}^{2+}$ ] and **4** [ $\text{Mn}^{2+}$ ] are isomorphous and isostructural with the previously reported crystal structure of the  $\text{Ni}^{2+}$  analogue [23]. All these complexes are differing solely with respect to the metal ion and hence, crystal structure description of only **2** has been given in detail. This Zn-CP crystallizes in tetragonal space group  $P4_12_12$ . The asymmetric unit consists of one half of the metal cation, one  $\text{NO}_2^-$  anion and one half of the bipy molecule (Fig. 3). The CCF of **2** is given as  $\text{AB}^2_3$ , where B corresponds to nitrito and bipy ligands. Each  $\text{Zn}^{2+}$  ion is bridged with six neighbouring  $\text{Zn}^{2+}$  ions via four  $\mu_{1,3}$ -nitrito bridges and two bipy ligands giving rise to a robust 3-D coordination architecture [Fig. 4(a)]. TOPOS analysis suggests a uninodal 6-c **jsm** underlying net [Fig. 4(b)] with point symbol  $(5^{10}.6^4.7)$ . All the 6-connected nodes present in the structure corresponds to Zn atoms which are linked with two bipy and four nitrito ligands. The natural tiling for the **jsm** net is isohedral [Fig. 5(a)], *i.e.* the net is formed by only one kind of tile with eight vertices, four faces, face symbol with ring type  $[5a^2.5b^2]$  and volume  $141.03\text{\AA}^3$ . A slightly distorted octahedral geometry around the  $\text{Zn}^{2+}$  center can be understood from the observed bonds angles being deviated from the expected value of  $90^\circ$ . The equatorial M–O distances for the complex were found to be  $2.175(2)\text{\AA}$  and  $2.157(2)\text{\AA}$ . A bit shorter M–N distances [ $2.105(2)\text{\AA}$  and  $2.117(2)\text{\AA}$ ] compared to the equatorial M–O distances suggest that the octahedral geometry is little compressed along the axial direction. These values are pretty close to those observed for the isostructural species  $[\text{Ni}(\text{bipy})(\text{NO}_2)_2]_n$  [23], being  $[2.124(5)\text{\AA}$  and  $2.126(5)\text{\AA}]$  and  $[2.051(8)\text{\AA}$  and  $2.063(7)\text{\AA}]$  for M–O and M–N distances respectively. Quite interestingly, the polymeric extension along the

crystallographic  $c$ -axis through the nitrito-bridges may be viewed as double-stranded helical chains as illustrated in Fig. 5(b). The *trans* bridging  $\text{NO}_2^-$  ligands are coordinated to the  $\text{Zn}^{2+}$  ion with a significantly twisted conformation having a dihedral angle of  $89.1(2)^\circ$ , indicating that they are almost perpendicular to each other. In fact, this conformational twist may be responsible for the formation of double helical chains in the crystal structure of the compound in the solid state. It is important to note that the  $\text{NO}_2^-$  anion in **1-4** functions as a bridging spacer *via* both the O-atoms. Considering the coordination abilities of the nitrite anion, this bridging ( $\mu$ -O,O'-nitrito) coordination mode in these  $\text{M}^{2+}$  complexes may be viewed as rare and rather unique. Structural similarity among these three complexes can be evaluated by using a method developed by Fabian and Kalman [54]. The observed unit cell similarity index ( $\Pi$ ) and also the mean elongation value ( $\epsilon$ ) for the pairs of structures (**2** & **3**,  $\Pi = 0.0196$ ,  $\epsilon = 0.020$ ; **3** & **4**,  $\Pi = 0.0063$ ,  $\epsilon = 0.0036$ ; **2** & **4**,  $\Pi = 0.0132$ ,  $\epsilon = 0.0166$ ) are quite close to zero, indicating the isomorphous nature of the complexes.

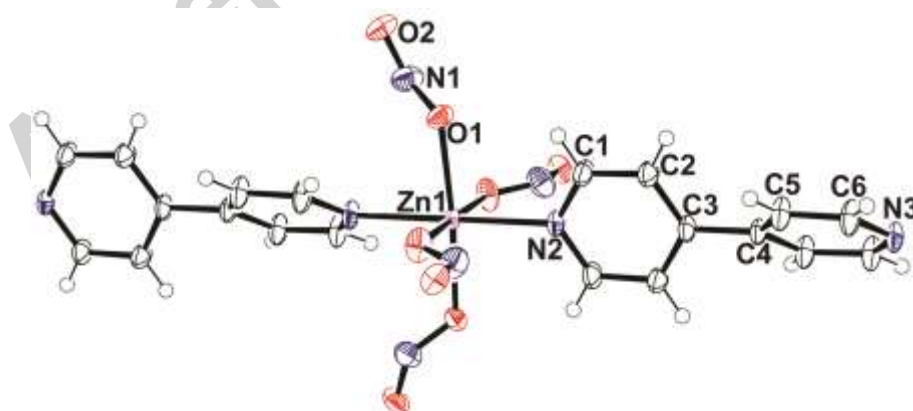


**Figure 3** ORTEP diagram with 50% probability ellipsoid showing the metal coordination of the polymeric species **2**.

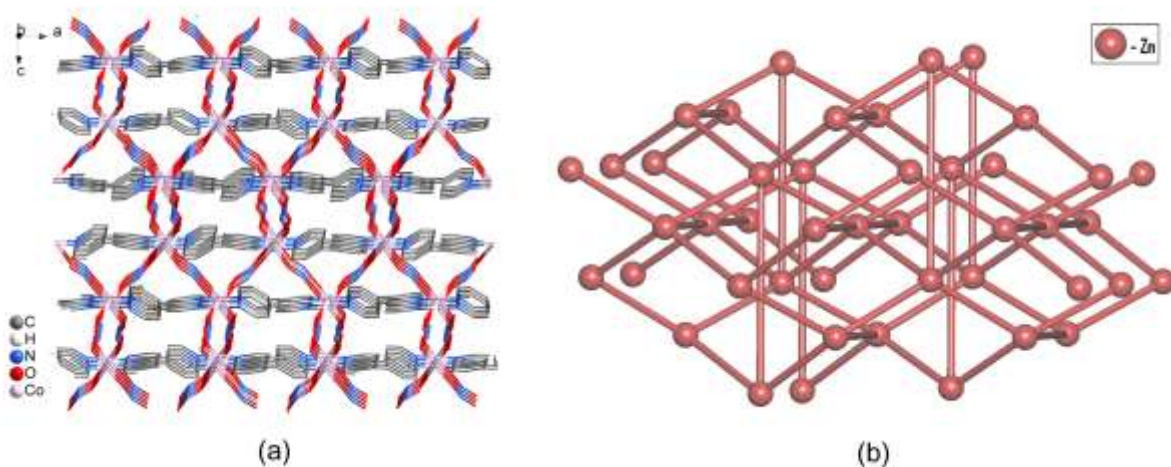


**Figure 4** a) A representation of **2** showing an extended 3-D structure *via* the coordination of Zn(II) ions with NO<sub>2</sub><sup>-</sup> and bipy ligands b) fragment of the six-connected **jsm** net.

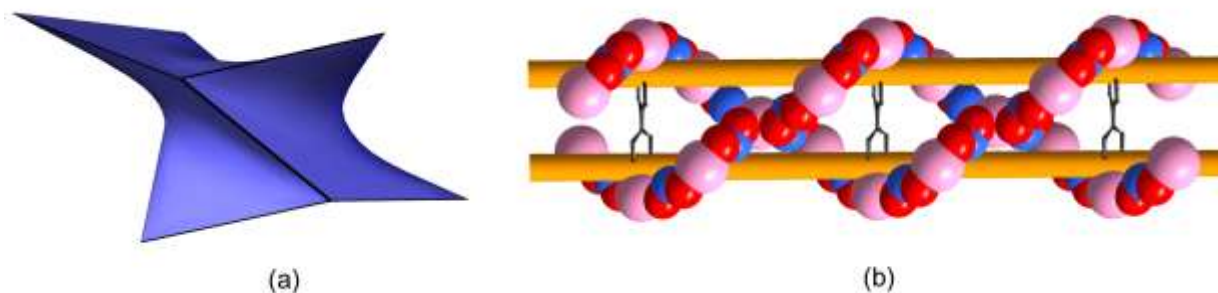


**Figure 5** a) The isohedral tiling of **jsm** net b) Double stranded helical structure of **2**

### 3.3 Powder X-ray diffraction behaviour

All the observed peaks in the experimental powder patterns of **2-4** are seen in the powder pattern calculated on the basis of structural results obtained from single-crystal data. A comparison of experimental PXRD patterns along with the calculated pattern of **2** is shown in Fig. 6. The close similarity between observed and calculated XRD patterns suggests the purity of crystalline bulk sample and also the veracity of the structure described by us. Powder XRD data with *hkl* indices

for the prominent lines have been determined by comparing the two patterns. Furthermore, nearly super-imposable PXRD patterns of the complexes **2-4** confirm their structural analogy.

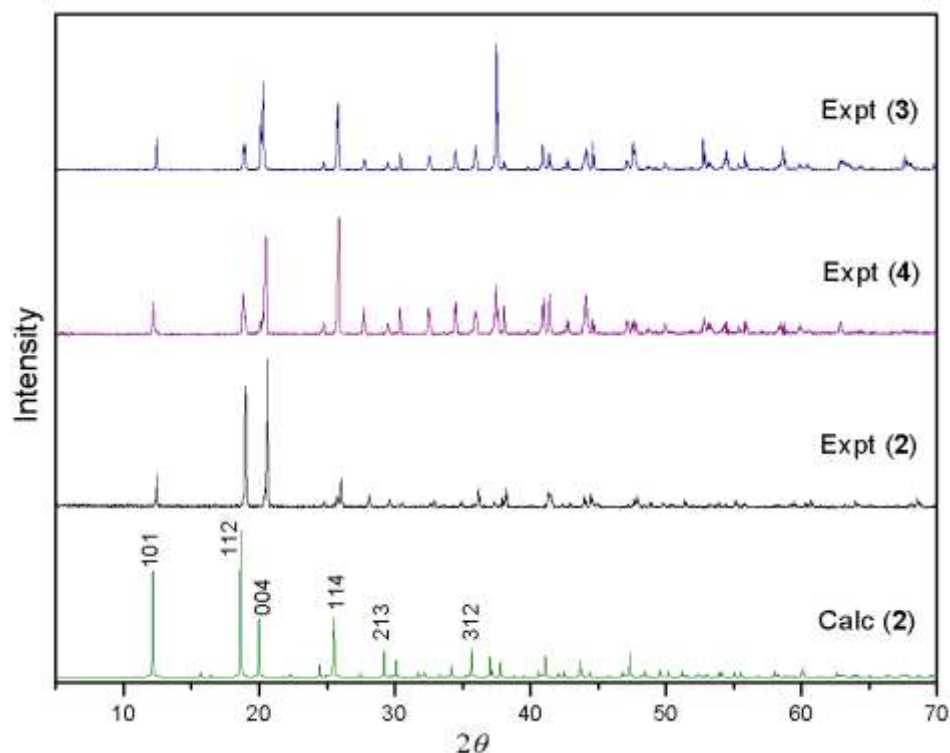


**Figure 6** Experimental powder XRD patterns of **2-4** with the simulated pattern of **2**.

### 3.4 Spectral Properties

#### 3.4.1 FT-IR and Raman spectroscopy

The Infrared and Raman spectra of the crystalline solids, **1-4** have been measured and are given together with tentative assignments of the bands in Table 2. Coincidence of Raman and Infrared frequencies has been observed for all the four compounds. The characteristic intra-ligand vibrations of NO<sub>2</sub> group [55-59] viz.  $\nu_{\text{sym(N-O)}}$  stretching and  $\delta_{\text{(NO}_2\text{)}}$  bending modes of the compounds were observed at expected positions, being 1352-1389 cm<sup>-1</sup> and 774-777 cm<sup>-1</sup> respectively. The skeletal vibration mode,  $\nu_{\text{(M-ONO)}}$  stretching were found at

relatively low frequencies and are shifted from one another. This frequency shift can probably be explained on the basis of Badger's rule [60-62] that relates the shifting vibrational frequencies with metal-ligand bond lengths. That is, increase in bond strength leads to corresponding frequency increase and vice versa. The M–Ligand(–ONO) bond distances and their corresponding vibrational frequencies of **1-4** are summarized in Table 3. On the other hand, the vibrations related to the bipy ligand are spreaded over the whole spectra, are similar to those of free bipy itself and slightly shifted in the solid compounds to a higher frequency.

**Table 2.** FT-IR and Raman frequencies of **1-4** with tentative assignment of bands.

		Frequency (cm <sup>-1</sup> )						Assignment	
		<b>1</b>		<b>2</b>		<b>3</b>			<b>4</b>
R	IR	R	IR	R	IR	R	IR	R	IR
167	-	126	-	130	-	117	-		$\nu(\text{M-ONO})$
774	-	777	-	775	-	774	-		$\delta(\text{NO}_2)$
1358	-	1355	1389	1352	1389	1353	1352		$\nu_{\text{sym}}(\text{N-O})$
-	-	403	-	401	-	396	-		ring breathing
-	-	661	637	659	635	659	658		ring breathing
-	-	1026	1015	1023	1013	1019	1004		ring breathing
-	-	1086	1090	1084	1090	1084	1076		$\nu(\text{C-C}), \nu(\text{C-N}), \delta(\text{C-H})$
-	-	1244	1221	1243	1221	1241	1221		$\delta(\text{C-H})$
-	-	1315	1350	1314	1348	1312	1352		ring breathing, $\delta(\text{C-H})$
-	-	1526	1558	1524	1560	1523	1533		$\nu(\text{C-C}), \nu(\text{C-N})$
-	-	1630	1611	1627	1609	1625	1603		$\nu(\text{C-C})$

R, Raman; IR, Infrared.

**Table 3.** Observed M-O vibrational frequencies (cm<sup>-1</sup>) and their bond distances (Å) for the **1-4**

Compound	$\nu_{(\text{M-ONO})}$ sym. stretch	M–O bond lengths
[Zn(NO <sub>2</sub> ) <sub>2</sub> (H <sub>2</sub> O) <sub>2</sub> ] <sub>n</sub> <b>1</b>	167 $\nu_{(\text{Zn-ONO})}$	2.070(2)
[Co(bipy)(NO <sub>2</sub> ) <sub>2</sub> ] <sub>n</sub> <b>3</b>	130 $\nu_{(\text{Co-ONO})}$	2.157(2)
[Zn(bipy)(NO <sub>2</sub> ) <sub>2</sub> ] <sub>n</sub> <b>2</b>	126 $\nu_{(\text{Zn-ONO})}$	2.175(2)
[Mn(bipy)(NO <sub>2</sub> ) <sub>2</sub> ] <sub>n</sub> <b>4</b>	117 $\nu_{(\text{Mn-ONO})}$	2.229(2)

### 3.4.2 UV-vis spectroscopy

The TD-DFT calculated UV-vis spectra of the cobaltous compound (**3**), is in very good agreement with the experimental solid state spectra (Fig. 7). The peak positions are almost similar to that of the experimental values; however, there is a slight decrease in the intensity of the calculated spectra. The peak at 490 nm (oscillator strength  $f = 0.032$ ) is assigned to the transition from HOMO-4 to LUMO+1 (Fig. 8). The HOMO-4 of the complex contains the metal  $d_{xy}$  orbital while the LUMO+1 consists of  $\pi^*$  orbitals of  $\text{NO}_2$  ligand. The transition at 990 nm (oscillator strength  $f = 0.022$ ) is mainly assigned to the transition from HOMO-2 having contribution from metal  $d_{yz}$  orbital to LUMO+1. The peak at 1220 nm (oscillator strength  $f = 0.057$ ) is mainly assigned to the HOMO to LUMO transition. The HOMO of the complex consists of the metal  $d_{zx}$  orbital with nonbonding electrons at the O-atoms of the  $\text{NO}_2$  group while the LUMO is mainly the  $\pi^*$  orbital centered at the  $\text{NO}_2$  group.

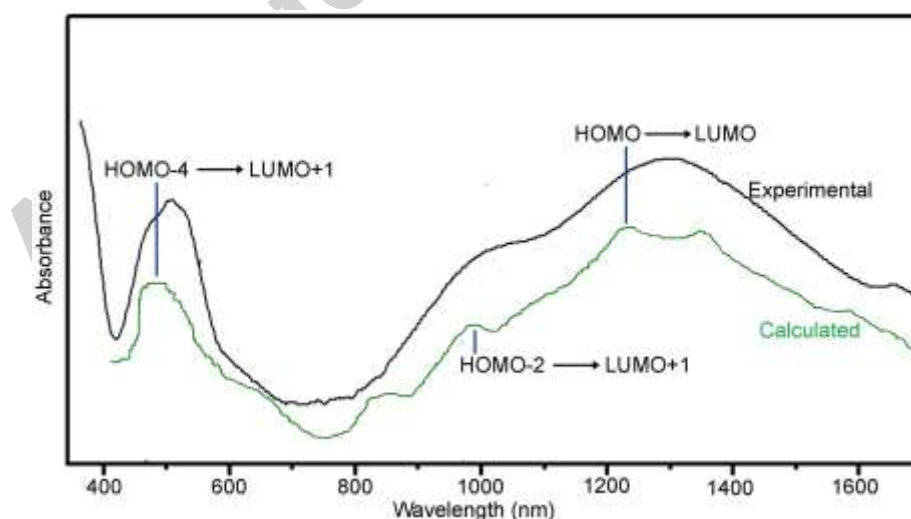


**Figure 7** The observed (black) and TD-DFT calculated (green) UV-vis spectra of **3**.

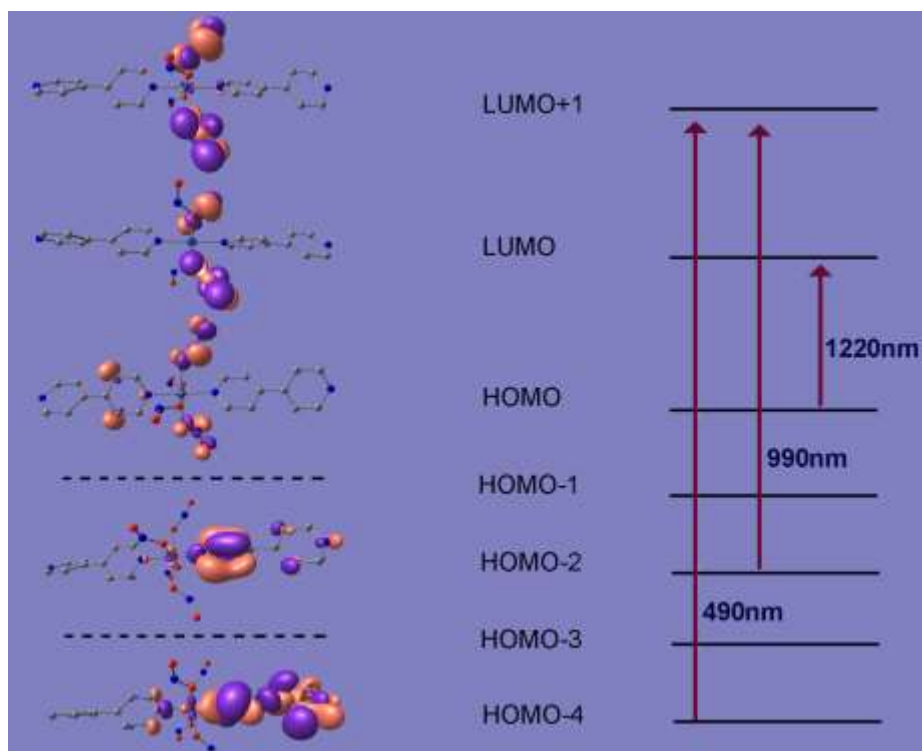


**Figure 8** Frontier Molecular Orbitals (FMOs) of **3** with the assigned electronic transitions.

### 3.5 Thermogravimetric analysis

TG analysis (Fig. 9) shows that compound **1** undergoes a combined weight loss of 35.03% for the expulsion of two aqua ligands along with a molecule of NO which is close to the calculated loss of 34.19% occurring at  $\sim 195$  °C. In the subsequent step, the species releases one NO<sub>2</sub> molecule (Calc. wt loss = 23.83%, Obs. wt loss = 25.01%) leaving ZnO as the final residue. Compounds **2** & **4** undergo one-step decomposition at  $\sim 260$  °C with the weight loss of 72.86% (Calculated value = 74.0%) and 79.96% (Calculated value = 78.21%) to produce ZnO and Mn<sub>3</sub>O<sub>4</sub> respectively. In case of **3**, the release of organic matters (Calc. wt loss = 73.9%, Obs. wt loss = 73.56%) took place in an unidentified manner and the final product was identified as Co<sub>3</sub>O<sub>4</sub>. While the gaseous products have not been experimentally identified by us, the observed PXRD pattern confirms the identity of the residue [Fig. 3 (a-c) in ESI]. This pathway is however

tentative because it has been proposed only on the basis of observed weight losses. Nevertheless, the TG results clearly suggest that the polymeric species **1-4** can be thermolysed to produce their respective metal oxides as pure products at relatively low temperature.

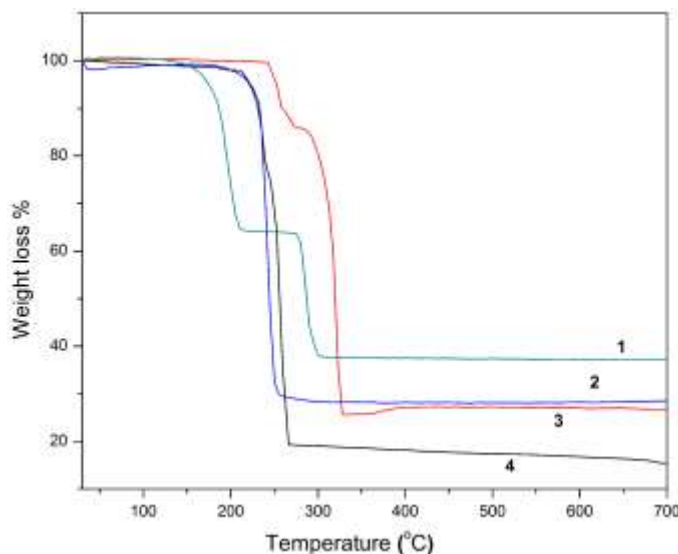
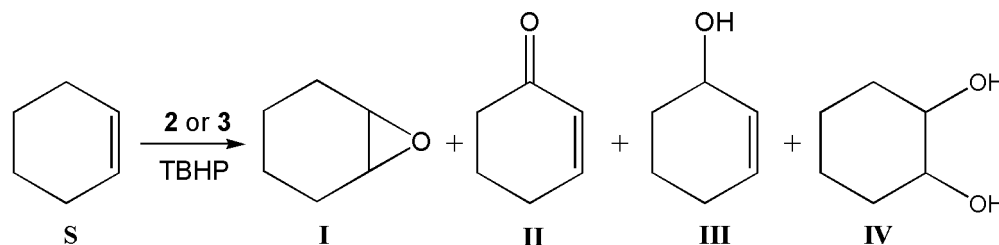


**Figure 9** Thermogravimetric curves obtained for compounds **1-4** under N<sub>2</sub> atmosphere.

### 3.6 Catalytic properties

To access the catalytic properties, the polymers **2** and **3** were employed in the oxidation of cyclohexene (**S**) using TBHP as oxidant in acetonitrile (Scheme 2) medium. Results of these reactions indicate that maximum conversions of cyclohexene were obtained at 8 hrs (48.8% conv.) and 10 hrs (62.4% conv.) for the catalysts **2** & **3** respectively and are presented in Fig. 10. Oxidation of cyclohexene in presence of **2** produces cyclohexene epoxide (**I**) as the major product and 2-cyclohexen-1-one (**II**), 2-cyclohexenol (**III**) and cyclohexane-1,2-diol (**IV**) in small yields which are evidently identified using GC by comparison with standards. On the other hand with catalyst **3**, the selectivity towards the product **II** & **III** were found to be more compared to the rest. Reusability of compound **2** as a catalyst has been checked (Fig. 4 ESI). The catalyst was

recovered by centrifugation, washed with methanol to remove the contaminants, dried properly and reused in the catalytic run. The similar procedure was performed upto 4<sup>th</sup> run and it was observed that the activity was decreased however, a little bit cyclohexane oxide selectivity was increased.



Scheme 2

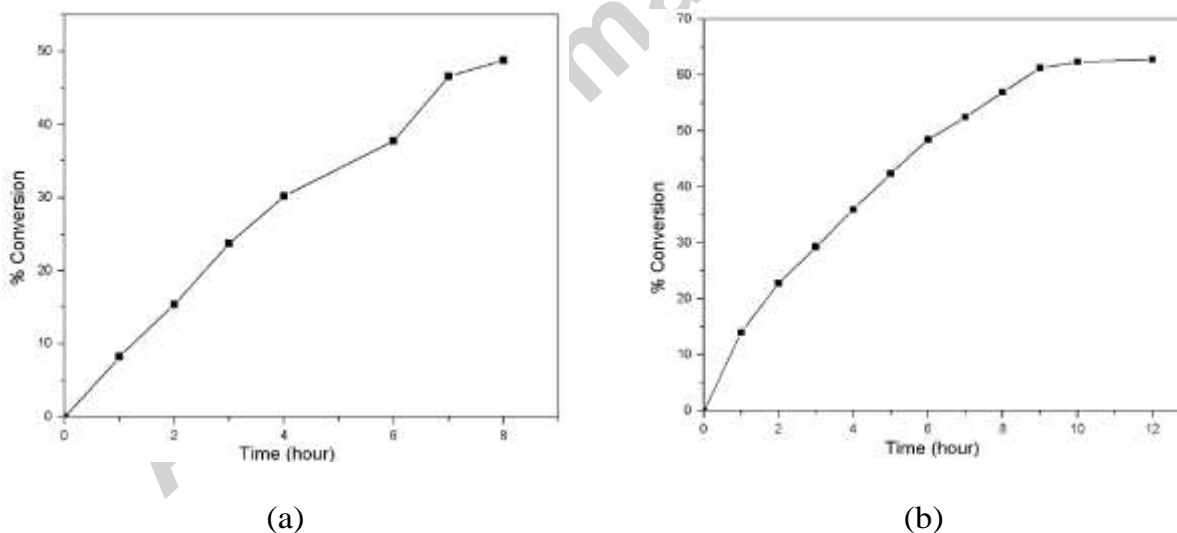


**Figure 10** Cyclohexene conversion with respect to time using (a) **2** and (b) **3** at 60 °C.

#### 4 Conclusion

Four new nitrito-bridged coordination polymers, **1-4** were constructed from nitrate ( $\text{NO}_3^-$ ) salts using DMF as the reducing solvent. The *in-situ* reduction of  $\text{NO}_3^-$  to  $\text{NO}_2^-$  (using DMF) during the syntheses of these CPs was established by theoretical calculations. Two crystallographically as well as compositionally distinct Zn(II) ions in **1** are bridged through  $\mu_{1,3}\text{-NO}_2^-$  anions generating a 3-D polymeric structure and can be rationalized as a 6-c uninodal **mab** underlying net. In the crystal structures of **2-4**, the bridging nitrito ligands are twisted in such a way that it results in double stranded helical chains. These isostructural CPs are extending in 3-D with a uninodal 6-c **jsm** underlying net. Oxidation of cyclohexene in presence of **2** and **3** shows maximum conversion of 48.8% and 62.4% producing cyclohexene epoxide and 2-cyclohexen-1-one respectively as the major products.

#### Acknowledgements

Financial support from Department of Science and Technology, India (FASTTRACK Grant No. SB/FT/CS-047/2013) is gratefully acknowledged. The authors also thank Department of Instrumentation and USIC, Gauhati University, Guwahati and Department of Chemistry, Jadavpur University, Kolkata for providing with the X-ray diffraction data.

#### References

- [1] M. L. Foo, R. Matsuda, S. Kitagawa, Chem. Mater. 26(1) (2014) 322.
- [2] X.-M. Lian, W. Zhao, X.-L. Zhao, J. Solid Stat. Chem. 200 (2013) 265.
- [3] D. Bradshaw, J. B. Claridge, E. J. Cussen, T. J. Prior, M. J. Rosseinsky, Acc. Chem. Res. 38 (2005) 273.

- [4] S. Zang, Y. Su, Y. Song, Y. Li, Z. Ni, H. Zhu, Q. Meng, *Cryst. Growth Des.* 6 (2006) 2369.
- [5] G. H. Dahl, B. P. Block, *Inorg. Chem.* 6 (1967) 1439.
- [6] Y.-B. Dong, M. D. Smith, H.-C. zur Loye, *Inorg. Chem.* 39 (2000) 4927.
- [7] P. Liang, C. Zhang, X. Duan, H. Sun, S. Liu, M. O. Tade, S. Wang, *ACS Sustainable Chem. Eng.* 5(3) (2017) 2693.
- [8] A. H. Chughtai, N. Ahmad, H. A. Younus, A. Laypkov, F. Verpoort, *Chem. Soc. Rev.* 44 (2015) 6804.
- [9] J.-R. Li, Y. Ma, M. C. McCarthy, J. Sculley, J. Yu, H.-K. Jeong, P. B. Balbuena, H. C. Zhou, *Coord. Chem. Rev.* 255 (2011) 1791.
- [10] C. Janiak, *Dalton Trans.* (2003) 2781.
- [11] T.-H. Park, K. A. Cychosz, A. G. Wong-Foy, A. Dailly, A. J. Matzger, *Chem. Commun.* 47 (2011) 1452.
- [12] L. Wen, L. Zhou, B. Zhang, X. Meng, H. Qu, D. Li, *J. Mater. Chem.* 22 (2012) 22603.
- [13] S. Sato, A. Ishii, C. Yamada, J. Kim, C. H. Song, A. Fujiwara, M. Takata, M. Hasegawa, *Polymer Journal* 47 (2015) 195.
- [14] X.-Y. Dong, C.-D. Si, Y. Fan, D.-C. Hu, X.-Q. Yao, Y.-X. Yang, and J.-C. Liu, *Cryst. Growth Des.* 16(4) (2016) 2062.
- [15] S. Kitagawa, R. Kitaura, S.-I. Noro, *Angew. Chem. Int. Ed.* 43 (2004) 2334.
- [16] M. L. Foo, R. Matsuda and S. Kitagawa, *Chem. Mater.* 26 (2014) 310.
- [17] R. Haldar, T. K. Maji, *CrystEngComm* 15 (2013) 9276-9295.
- [18] T. Liu, Y.-H. Chen, Y.-J. Zhang, Z.-M. Wang, S. Gao, *Inorg. Chem.* 45 (2006) 9148.
- [19] M. A. Hitchman, G. L. Rowbottom, *Coord. Chem. Rev.* 42 (1982) 55.
- [20] W. B. Tolman, *Inorg. Chem.* 30 (1991) 4880.
- [21] T. M. Rajendiran, C. Mathonière, S. Golhen, L. Ouahab, O. Kahn, *Inorg. Chem.* 37 (1998) 2651.
- [22] C. Diaz, J. Ribas, R. Costa, J. Tercero, Salah M. El Fallah, X. Solans, M. Font-Bardía, *Eur. J. Inorg. Chem.* (2000) 675.
- [23] V. Vo, Y. Kim, N. V. Minh, C. S. Hong, S.-J. Kim, *Polyhedron*, 28 (2009) 1150.
- [24] H. A. Habib, J. Sanchiz, C. Janiak, *Dalton Trans.* (2008) 1734.
- [25] D. Singh, C. M. Nagaraja, *Cryst. Growth Des.* 15(7) (2015) 3356;
- [26] Y. Wu, G. -P. Yang, X. Zhou, J. Li, Y. Ning, Y.-Y. Wang, *Dalton Trans.* 44 (2015) 10385.
- [27] B. Conerney, P. Jensen, P. E. Kruger, B. Moubaraki, K. S. Murray, *CrystEngComm* 5(80) (2003) 454.
- [28] A. J. Fletcher, E. J. Cussen, D. Bradshaw, M. J. Rosseinsky, K. M. Thomas, *J. Am. Chem. Soc.* 126 (2004) 9750.

- [29] B. D. Wagner, G. J. McManus, B. Moulton, M. J. Zaworotko, *Chem. Commun.* (2002) 2176.
- [30] O. M. Yaghi, H. Li, T. L. Groy, *Inorg. Chem.* 36 (1997) 4292.
- [31] M. Kondo, T. Yoshitomi, K. Seki, H. Matsuzaka, S. Kitagawa, *Angew. Chem., Int. Ed. Engl.* 36 (1997) 1725;
- [32] C. J. Kepert, M. J. Rosseinsky, *Chem. Commun.* (1999) 375.
- [33] M. Fujita, Y. J. Kwon, S. Washizu, K. Ogura, *J. Am. Chem. Soc.* 116 (1994) 1151.
- [34] J. Lu, T. Paliwala, S. C. Lim, C. Yu, T. Niu, A. J. Jacobson, *Inorg. Chem.* 36 (1997) 923;
- [35] L.-M. Zheng, X. Feng, K.-H. Lii, H.-H. Song, X.-Q. Xin, H.-K. Fun, K. Chinnakali, I. A. Razak, *J. Chem. Soc., Dalton Trans.* (1999) 2311;
- [36] D. Hagrman, R. P. Hammond, R. Haushalter, J. Zubieta, *Chem. Mater.* 10 (1998) 2091.
- [37] A. D. Becke, *J. Chem. Phys.* 98 (1993) 5648.
- [38] C. Lee, W. Yang, R. G. Parr, *Phys Rev B Condens Matter.* 37 (1988) 785.
- [39] J. Tomasi, M. Persico, *Chem. Rev.* 94 (1994) 2027.
- [40] Neese F. ORCA—An ab Initio, Density Functional and Semiempirical Program Package, Version 3.0.2. Bonn: University of Bonn; (2008).
- [41] SMART/SAINT: Bruker AXS Inc., Madison, Wisconsin, USA, 2004.
- [42] G. M. Sheldrick, *Acta Cryst. A*64 (2008) 112.
- [43] L. Farrugia, *J. Appl. Cryst.* 32 (1999) 837.
- [44] M. N. Burnett, Johnson, C.K. ORTEP-III: Oak Ridge Thermal Ellipsoid Plot for Crystal Structure Illustrations, Oak Ridge National Laboratory Report ORNL-6895, 1996.
- [45] L. Farrugia, ORTEP-3 for Windows: ver. 1.08, *J. Appl. Cryst.* 30 (1977) 565.
- [46] A. L. Spek, *Acta Cryst. A*46 (1990) C-34.
- [47] K. Brandenburg, Diamond: Ver. 3.1f, Crystal Impact GbR, Bonn, Germany, 2008.
- [48] Mercury: ver. 1.4.2, CCDC, Cambridge, UK, 2007.
- [49] W. Kraus, G. Nolze, PowderCell for Windows, Ver. 2.4. 2000, Berlin: Federal Institute for Materials Research and Testing., Berlin, Germany.
- [50] I. Pastoriza-Santos, L. M. Liz-Marzán, *Langmuir*, 15 (1999) 948.
- [51] V. N. Serezhkin, A. V. Vologzhanina, L. B. Serezhkina, E. S. Smirnova, E. V. Grachova, P. V. Ostrovac, M. Yu. Antipin, *Acta Cryst. B*65 (2009) 45.
- [52] V. A. Blatov, A. P. Shevchenko, D. M. Proserpio, *Cryst. Growth Des.* 14 (2014) 3576.
- [53] J. Bernstein, R.E. Davis, L. Shimoni, N.-L. Chang, *Angew. Chem. Int. Ed. Engl.* 34 (1995) 1555.
- [54] L. Fábíán, A. Kálmán, *Acta Cryst. B*55 (1999) 1099.

- [55] K. Kanamori, A. Shimizu, H. Sekino, S. Hayakawa, Y. Seki, K. Kawai, J. Chem. Soc. Dalton Trans. 1988, 1827.
- [56] D. M. L. Goodgame, M. A. Hitchman, Inorg. Chem. 6(4) (1967) 813.
- [57] B. J. Hathaway, R. C. Slade, J. Chem. Soc. Inorg. Phys. Theor. (1966) 1485.
- [58] I. E. Grey, M. A. Hitchman, G. L. Rowbottom, N. V. Y. Scarlett, J. Wilson, J. Chem. Soc. Dalton Trans. (1994) 595.
- [59] B. J. Hathaway, R. C. Slade, J. Chem. Soc. Inorg. Phys. Theor. 1967, 952.
- [60] R. M. Badger, J. Chem. Phys. 2 (1934) 128.
- [61] R. M. Badger, J. Chem. Phys. 3 (1935) 227.
- [62] J. Cioslowski, G. Liu, R. A. M. Castro, Chem. Phys. Lett. 331 (2000) 497.

## Graphical abstract

New nitrito-bridged coordination polymers of formulation  $[\text{Zn}(\text{NO}_2)_2(\text{H}_2\text{O})_2]_n$  and  $[\text{M}(\text{bipy})(\text{NO}_2)_2]_n$  [M= Zn, Co, Mn] were synthesized under solvothermal condition. Theoretical calculations established that there is *in-situ* reduction of  $\text{NO}_3^-$  to  $\text{NO}_2^-$  (using DMF) during the syntheses of these CPs. The catalytic activity for oxidation of cyclohexene was found to be very good.

